# i-Rheo *GT*: Transforming from time- to frequency-domain without artefacts

Manlio Tassieri,[*,†] Jorge Ramírez,[*,‡] Nikos Ch. Karayiannis,[¶] Sathish K. Sukumaran,[§] and Yuichi Masubuchi[‖]

†*Division of Biomedical Engineering, School of Engineering, University of Glasgow, G12 8LT, U.K.*

‡*Departamento de Ingeniería Química Industrial y Medio Ambiente, Universidad Politécnica de Madrid, José Gutiérrez Abascal 2, 28006 Madrid, Spain.*

¶*Institute for Optoelectronics and Microsystems (ISOM), Universidad Politécnica de Madrid, José Gutiérrez Abascal 2, 28006 Madrid, Spain.*

§*Graduate School of Organic Materials Science, Yamagata University, Yonezawa 992-8510, Japan.*

‖*Department of Materials Physics, Nagoya University, Nagoya 464-8603, Japan.*

E-mail: Manlio.Tassieri@glasgow.ac.uk; jorge.ramirez@upm.es

**Abstract**

We present a new analytical tool for educing the frequency-dependent complex shear modulus of materials from computer-aided numerical simulations of their time-dependent shear relaxation modulus; without the need of preconceived models. The rheological tool is presented in the form of an open access executable named 'i-Rheo ***GT***', enabling its use to a broad scientific community. Its effectiveness is corroborated by analysing the dynamics of *ideal* single mode Maxwell fluids, and by means of a direct

comparison with both bulk-rheology measurements and coarse-grained molecular dynamics simulations data transformed via a generalised Maxwell model. When adopted to transform atomistic molecular dynamics simulations data, the unbiased nature of the tool reveals *new insights* into the materials' linear viscoelastic properties, especially at high frequencies, where conventional tools struggle to interpret the data and molecular dynamics simulations actually provide their most statistically accurate predictions. The wideband nature of i-Rheo ***GT*** offers the opportunity to better elucidate the link between materials' topologies and their linear viscoelastic properties; from atomic length scales at frequencies of the order of THz, up to mesoscopic length scales of molecular diffusion phenomena occurring over time scales of hours.

# 1 Introduction

"*The nature of matter is to be found in the structure and motion of its constituent building blocks, and the dynamics is contained in the solution to the N-body problem. Given that the classical N-body problem lacks a general analytical solution, the only path open is the numerical one*".[1]

In the field of rheology, it has been shown[2–4] that the mechanical properties of (complex) materials are governed by the *ensemble* of inter- and intra-molecular interactions occurring at different time- and length-scales (such as the entanglements between polymer chains or their diffusion). This indeed is a classical N-body problem, for which a full analytical solution is still yearned. However, despite the multitude and the complexity of molecular interactions, rheologists have successfully drawn 'simplistic' (i.e., coarse-grained (CG)[5]) representations of materials' topology (e.g., the tube model[3]) that have substantially reduced the number of variables required to educe the materials' viscoelastic properties by means of computer-aided numerical simulations. Nevertheless, despite their effectiveness in interpreting many experimental results,[6] CG models lack of microscopic interpretations of molecular dynamics because of their inherent discrete nature.[7] For this reason and concurrently with the contin-

uous development of powerful central processing units (CPUs) and graphics processing units (GPUs), rheologists have been encouraged to embark on molecular dynamics (MD) simulations based on atomistic models. These indeed are potentially able to predict the materials' dynamics over much wider time and length scales; i.e., from atomic bond fluctuations, occurring at picoseconds time scales, to molecular diffusion in glassy materials, a process that may take several months before a distance of the order of the molecule dimension is achieved.

In linear rheology, a common aim of MD simulation studies is the evaluation of the time-dependent material's shear relaxation modulus $G(t)$ for a discrete number of timestamps, within a finite observation time window. This because $G(t)$ embodies, without disclosing at once, the material's linear viscoelastic (LVE) properties that are instead fully revealed by the frequency-dependent material's complex shear modulus $G^*(\omega)$. The latter is a complex number whose real and imaginary parts provide quantitative information on the elastic and viscous nature of the material, respectively. Notably, these two moduli are in principle simply related to each other by means of the Fourier transform of the time derivative of $G(t)$ (i.e., Eq. 3), whose computation given a discrete set of data is at the heart of this article. In this regard, it has been shown[8] that the evaluation of the Fourier transform of a sampled function, given only a finite set of data points over a finite time domain, is non-trivial[9–14] since interpolation and extrapolation from those data can yield artefacts that lie within the bandwidth of interest. In order to overcome such an issue, it has become almost a standard procedure to convert the outcomes of MD simulation (i.e., $G(t)$) by means of a Generalised Maxwell model (i.e., a finite sum of weighted single exponentials, each identifying a characteristic relaxation time of the system), which has a straightforward Fourier transform. However, this analytical procedure presents some drawbacks: (i) it leaves some uncertainties related to the accuracy and non-uniqueness of the fitting procedure; (ii) it is affected by the operator's choice of the number of Maxwell modes; (iii) at long times it is based on *"The strong assumption...that after the last exponent the relaxation is exponential"*[1]; (iv) because of

[1] Alexei Likhtman, private communication.

points (i) & (ii), it commonly leads to ignore interesting information hidden in the short-time behaviour of $G(t)$, where fast modes take control of the material's dynamics.[7,15] Notably, all the above issues are discarded by the analytical tool introduced in this work.

We present a new rheological '*tool*' to evaluate the materials' LVE properties over the widest range of experimentally accessible frequencies from (atomistic and coarse-grained) molecular dynamics simulations, without the need of preconceived models. This is achieved by evaluating the Fourier transforms of raw simulation data describing the temporal behaviour of $G(t)$ by means of the analytical method introduced by Tassieri *et al.*[8] The latter has been implemented into a new open access executable named 'i-Rheo ***GT***' and its effectiveness has been corroborated both by analysing the dynamic response of model systems (i.e., single mode Maxwell fluids) and by direct comparison with both bulk-rheology experimental data and coarse-grained molecular dynamics simulations data transformed via a generalised Maxwell model, as described in sections 3.1 and 3.2, respectively. Moreover, in section 3.3, we fully exploit the results of previous rheological studies,[7] where (i) informative MD simulations of $G(t)$ were misinterpreted and (ii) the related materials' high frequency response partially discarded because of the absence of an effective tool for data analysis, as the one presented in this work. Finally, we demonstrate that, when i-Rheo ***GT*** is adopted to analyse the results obtained from atomistic molecular dynamics simulations, it offers the opportunity to gain *new insights* into the materials' LVE properties, especially at high-frequencies (i.e., in the glassy region and above), where conventional tools (e.g., Iris[2] or Reptate[3]) struggle to interpret the data and MD simulations actually provide their most statistically accurate predictions of $G(t)$; as described in section 3.4.

[2]Winter, H. H. , and M. Mours, IRIS Developments, http://rheology.tripod.com/ (2003).
[3]Likhtman, A.E. and J. Ramirez, http://reptate.com (2009)

# 2 Theoretical background

## 2.1 Linear rheology

In the time-domain, the LVE properties of a material are potentially fully embedded into its shear relaxation modulus, which is a function defined only for positive times (i.e., $\forall t \in [0, +\infty[$) because of *causality*. This is elucidated by means of the following constitutive equation of linear viscoelasticity in simple shear:[2]

$$\sigma(t) = \int_{-\infty}^{t} G(t - t')\dot{\gamma}(t')\mathrm{d}t' \tag{1}$$

where $\sigma(t)$ is the shear stress, $\dot{\gamma}(t)$ is the shear rate (i.e., the time derivative of the shear strain $\dot{\gamma}(t) = d\gamma(t)/dt$) and the integration is carried out over all past times $t'$ up to the current time $t$. From Equation 1 it follows that, for a material at thermodynamic equilibrium, if $t_0$ is the time at which a generic strain function is applied, then both sides of Equation 1 are different from zero only for $t' \geqslant t_0$. In this case, (i) for a purely elastic solid, Equation 1 becomes $\sigma(t) = G\gamma(t)$, with a time-indepented elastic shear modulus $G$ equal to a third of the Young's modulus of the material; whereas, (ii) for viscoelastic materials, their LVE properties are in theory fully embedded into the temporal behaviour of $G(t)$ $\forall t \geqslant 0$ (i.e., for all $t' \geqslant t_0 = 0$), *if and only if* the strain assumes the ideal form of either a unit *impulse* ($\delta(t)$) or a unit *step* ($u(t)$) function at time $t_0$.[2,16]

Nevertheless, even in the above mentioned two ideal cases, $G(t)$ is not able to reveal at once any viscoelastic parameter, unless a predetermined model is adopted *a priori*. By contrast, these properties are fully uncovered by the material's complex shear modulus:

$$G^*(\omega) = G'(\omega) + iG''(\omega) \tag{2}$$

where $\omega$ is the angular frequency, $i$ is the imaginary unit (i.e., $i^2 = -1$), $G'(\omega)$ and $G''(\omega)$ are the material storage (elastic) and loss (viscous) moduli, respectively. Moreover, the complex

modulus is simply related to the shear relaxation modulus by means of the following Fourier transform:

$$G^*(\omega) = \int_{-\infty}^{+\infty} \dot{G}(t) e^{-i\omega t} dt = i\omega \hat{G}(\omega) \tag{3}$$

where $\dot{G}(t)$ and $\hat{G}(\omega)$ are the time derivative and the Fourier transform of $G(t)$, respectively. Notice that, $G^*(\omega)$ is *time-invariant* and Equation 3 is valid whatever is the nature of the material under investigation.[2]

Despite the elementary appearance of Equation 3, its evaluation has revealed to be not a straightforward process.[9–13] This has driven rheologists to overcome such an issue by performing a best fit of $G(t)$ with a known function having a well defined Fourier transform, such as a generalised Maxwell model:

$$G(t) = \sum_{i=1}^{N} G_i e^{-t/\tau_i}, \quad with \quad \tau_i = \frac{\eta_i}{G_i} \tag{4}$$

where $G_i$ and $\eta_i$ are respectively the elastic and the viscous contribution of the $ith$ mode that identifies a characteristic relaxation time $\tau_i$ of the material. This is a very common analytical procedure that, despite its effectiveness, presents some downsides due to its tendency at *influencing* the outcomes; as already mentioned in the introduction and further discussed later in the paper.

At this point it is important to highlight that the above LVE framework (i.e., Equations 1 to 4) is a valid assumption as long as the system is at thermodynamic equilibrium (i.e., isothermal) for all the explored times. In real systems, this assumption may not be valid or at least not for all the explored frequencies. This is indeed a *dilemma* that is still a subject of studies in the field of polymer physics, where a method for identifying a frequency-crossover between the materials' isothermal dynamics at low frequencies and those adiabatic at high frequencies is *yet unknown*. However, it is expected that such (smooth) transition would occur at frequencies of the order of the fluctuations of the local structural units (bonds, angles and torsions); i.e., several decades away from the novel polymeric features

that we reveal in this work on the basis of a isothermal assumption; hence, the potential veracity of our findings. Nonetheless, it is germane to note that any comparison between the isothermal moduli obtained from MD simulations (e.g., either via i-Rheo ***GT*** or for that matter, any other analytical procedure) and the high-frequency experimental data must be performed with care, as the experiments are believed to probe the system under adiabatic conditions.[17,18]

## 2.2 Evaluating the Fourier transform of raw data

An analytical procedure for the evaluation of the Fourier transform of any generic function sampled over a finite time window was proposed by Evans *et al.*,[12,13] to convert creep compliance $J(t)$ (i.e., a *step*-stress measurement) into $G^*(\omega)$ directly, without the use of Laplace transforms or fitting functions. This method is based on the interpolation of the finite data set by means of a piecewise-linear function. In particular, the general validity of the proposed procedure makes it equally applicable to find the Fourier transform $\hat{g}(\omega)$ of any time-dependent function $g(t)$ that vanishes for negative $t$, sampled at a finite set of data points $(t_k, g_k)$, where $k = 1 \ldots N$, which extend over a finite range, and *need not* be equally spaced:[12]

$$-\omega^2 \hat{g}\left(\omega\right) = i\omega g(0) + \left(1 - e^{-i\omega t_1}\right) \frac{\left(g_1 - g(0)\right)}{t_1} + \\ + \dot{g}_\infty e^{-i\omega t_N} + \sum_{k=2}^{N} \left(\frac{g_k - g_{k-1}}{t_k - t_{k-1}}\right) \left(e^{-i\omega t_{k-1}} - e^{-i\omega t_k}\right) \tag{5}$$

where $\dot{g}_\infty$ is the gradient of $g(t)$ extrapolated to infinite time and $g(0)$ is the value of $g(t)$ extrapolated to $t = 0$ from above.

This method was improved by Tassieri *et al.*[8] while analysing microrheology measurements performed with optical tweezers.[14] The authors found that a substantial reduction in the size of the high-frequency artefacts, from which some high-frequency noise tends to spill over into the top of the experimental frequency range, can be achieved by an *over-sampling*

technique. The technique involves first numerically interpolating between data points using a standard non-overshooting cubic spline, and then generating a new, over-sampled data set, by sampling the interpolating function not only at the exact data points but also at a number of (equally-spaced) points in between. We remind that, over-sampling is a common procedure in signal processing and it consists of sampling a signal with a sampling frequency $f_s$ much higher than the Nyquist rate $2B$, where $B$ is the highest frequency contained in the original signal. A signal is said to be oversampled by a factor of $\beta \equiv f_s/(2B)$.[19]

## 2.3 Calculation of $G(t)$ from simulations

In equilibrium simulations, the shear relaxation modulus can be calculated by means of the linear-response theory expression:

$$G(t) = \frac{V}{k_B T} \langle \sigma_{xy}(t) \sigma_{xy}(0) \rangle \tag{6}$$

where $V$ is the system volume, $k_B$ is Boltzmann's constant, $T$ is the absolute temperature and $\sigma_{xy}$ is the shear component of the stress tensor. In Eq. 6, it is assumed that the average value of the shear stress at equilibrium is zero. Every time step, the stress tensor can be obtained from the classical virial definition:

$$\sigma_{\alpha\beta} = \frac{1}{V} \left( - \sum_i m_i v_{i\alpha} v_{i\beta} + \frac{1}{2} \sum_{i,j \neq i} r_{ij\alpha} f_{ij\beta} \right) \tag{7}$$

where $m_i$ and $v_i$ are the mass and velocity of particle $i$, respectively, $r_{ij}$ is the distance between particles $i$ and $j$, $f_{ij}$ is the force on particle $i$ due to particle $j$ and $\alpha, \beta = x, y, z$. At equilibrium, if the system is isotropic, the accuracy of Eq. 6 can be improved considerably

by averaging over all possible orientations of the reference system of coordinates:

$$G(t) = \frac{V}{5k_BT}\left[\langle\sigma_{xy}(t)\sigma_{xy}(0)\rangle + \langle\sigma_{yz}(t)\sigma_{yz}(0)\rangle + \langle\sigma_{zx}(t)\sigma_{zx}(0)\rangle\right] + \frac{V}{30k_BT}\left[\langle N_{xy}(t)N_{xy}(0)\rangle + \langle N_{yz}(t)N_{yz}(0)\rangle + \langle N_{zx}(t)N_{zx}(0)\rangle\right] \quad (8)$$

where $N_{\alpha\beta} = (\sigma_{\alpha\alpha} - \sigma_{\beta\beta})$ is the corresponding normal stress difference.

Equation 8 can be evaluated by post-processing the simulated trajectories. As discussed below, in entangled polymers the value of the relaxation modulus at the plateau and terminal regions is typically orders of magnitude lower than its value at time $t = 0$. It is therefore important to accumulate enough data to grant good statistics that would allow to resolve those small values accurately. Ideally, one could store the stress tensor at each time step during the simulation, but that would lead to huge trajectory files and extremely slow post-processing operations. An alternative approach is to use a multiple-tau correlator,[20] that allows an efficient and fast evaluation of time correlation functions on the fly during simulations. This method has a very small impact on the efficiency of the simulation (less than 1%) and can be tuned to a desired level of accuracy.

# 3 Results and Discussions

Figure 1 shows the front panel of the executable i-Rheo ***GT***, which allows the evaluation of the material's complex shear modulus *via* Equation 3 by performing the Fourier transform of the shear relaxation modulus obtained from MD simulations. In particular, i-Rheo ***GT*** reads the raw data (i.e., $[t_k, G_k]$) in the form of a regular tab-separated text file (.txt) and generates a new oversampled set of data (with a sufficiently high value of $\beta \equiv f_s/(2AR) \gg \omega/AR$, usually $f_s \cong 10$ MHz); then, it applies Equation 5 to this new data set and returns the viscoelastic moduli of the system under investigation.

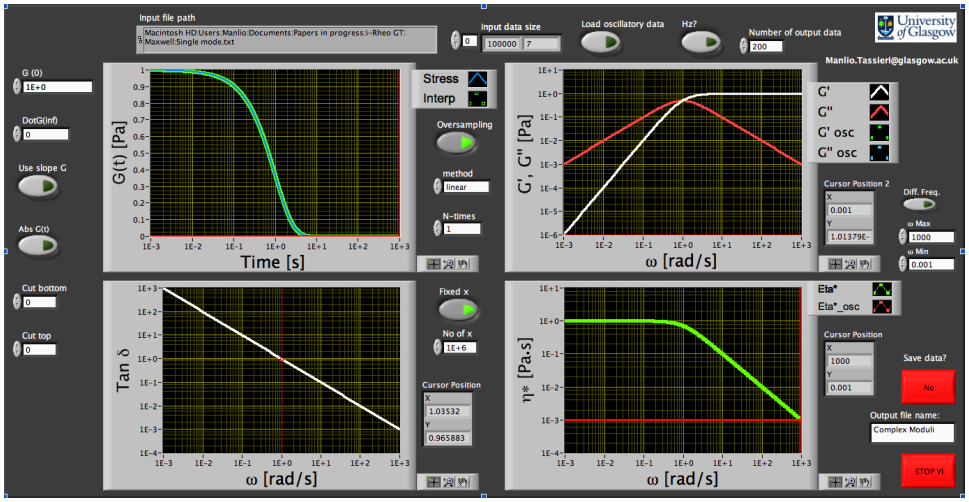


Figure 1: Front panel of the LabVIEW (National Instruments) executable 'i-Rheo ***GT***', which implements the analytical method introduced by Tassieri *et al.*[8] to evaluate the Fourier transform of the shear relaxation modulus $G(t)$ in Equation 3. The executable is free to download (together with the instructions) from the following link: `https://sites.google.com/site/manliotassieri/labview-codes`.

As mentioned before, Equation 5 requires two external inputs (i.e., $g(0)$ and $\dot{g}_\infty$) that in this case are given by the values of $G(t)$ at time $t = 0$ ($G(0)$) and of its gradient at time plus infinite ($\dot{G}_\infty$), respectively. Interestingly, while the first parameter is usually the most statistically accurate expected value obtained from MD simulations and it is governed by the thermodynamic conditions at equilibrium, the second often represents a *chimera*, especially in the case of systems characterised by very slow relaxation processes (e.g., macromolecules diffusion in highly concentrated solutions, such as actin filament networks[21–24]). This is because of the lengthy simulation process required to achieve statistically valid results that would better represent such slow dynamics, but also because of the costs of random-access memory (RAM) and CPUs necessary to accomplish them. Nevertheless, for the great majority of viscoelastic materials, $\dot{G}_\infty$ is expected to be equal to zero, which represents a key feature for the analytical approach adopted in this work. In particular, for viscoelastic fluids whose linear response is characterised by the existence of the terminal region at low frequencies (where $G'(\omega) \propto \omega^2$ and $G''(\omega) \propto \omega$ for $\omega \to 0$), the long-time behaviour of the shear relaxation modulus is expected to be: $G(t) \propto \exp(-t/\tau)$ for $t \to \infty$ and therefore $\|\dot{G}_\infty\| \to 0$

for $t \to \infty$. The same conclusion is achieved in the case of viscoelastic solids (e.g., gels and rubbers), for which $G(t)$ tends to the equilibrium shear modulus $G_0$ at long times.

The effectiveness of i-Rheo ***GT*** is hereby initially corroborated by analysing the dynamic response of ideal systems represented by single mode Maxwell fluids (section 3.1). Then, it is further validated by means of a direct comparison with conventional bulk-rheology measurements and MD simulations of coarse-grained models transformed by means of Reptate (section 3.2). Finally, the advantages of using i-Rheo ***GT*** are highlighted in section 3.3, where its contribution to the field of polymer physics is presented in the form of a better understanding of the materials' LVE properties, especially at high-frequencies, in the glassy region and beyond, where current methods strive to convert the data.

## 3.1 Single mode Maxwell fluids

Given the discrete nature of the molecular dynamic simulations' outcomes, with particular attention to those obtained from coarse-grained models (for which the very short-time behaviour of $G(t)$ is not accounted), we wish to introduce a new dimensionless parameter ($T_a$) to assess the efficacy of i-Rheo ***GT*** as a function of the *relative position* of the material's characteristic relaxation time $\tau$ to that of the experimental time window $[t_1, t_N]$:

$$T_a = \frac{Log(\tau/t_1)}{Log(t_N/t_1)} \tag{9}$$

where, in the case of computer-aided simulations, $t_1$ and $t_N$ are set by the 'unit-time step' and the 'duration' of the simulation, respectively. Whereas, in the case of mechanical measurements, these extremes are dictated by the acquisition rate (AR) of the instrument (i.e., $t_1 = 1/AR$) and the duration of the test, which is often identified by the time at which the measured signal hits the sensitivity of the instrument. The meaning of $T_a$ is very similar in spirit to that of the Deborah number[25] (defined as the ration between the material's characteristic *time of relaxation* and the *time of observation*), but it takes into account also the

existence of a 'finite' acquisition rate (i.e., of $t_1$) and therefore it can also assume negative values $\forall \tau < t_1$.

In order to better appreciate the implications of the parameters $\beta$, $T_a$ and $G(0)$ on the outcomes of the analytical method implemented in i-Rheo ***GT***, we have evaluated the Mean-Relative-Absolute-Error (MRAE) of both the real and imaginary parts of the calculated complex modulus (i.e., $G'_{iR}(\omega)$ and $G''_{iR}(\omega)$) with respect to their expected values in the case of a single mode Maxwell fluid (i.e., $G'_M(\omega)$ and $G''_M(\omega)$, whose well-known expressions are recalled in Eq. 11):

$$MRAE(\beta, T_a, G(0)) = \frac{1}{N}\sum_{n=1}^{N}\frac{|G'_{iR}(\omega_n) - G'_M(\omega_n)|}{G'_M(\omega_n)} \tag{10}$$

where $n = 1...N$ is the number of frequencies at which Eq. 10 is evaluated (here $N = 400$, with $\omega_n$ equally spaced on a logarithmic scale ranging from $1/t_N$ to $1/t_1$). A similar expression can be written for the viscous modulus with $G'_{iR}(\omega_n)$ and $G'_M(\omega_n)$ replaced by $G''_{iR}(\omega_n)$ and $G''_M(\omega_n)$, respectively. The complex modulus of a single mode Maxwell fluid is:

$$G^*_M(\omega) = \frac{(\omega_n\tau)^2}{1+(\omega_n\tau)^2} + i\frac{\omega_n\tau}{1+(\omega_n\tau)^2} \tag{11}$$

from which the expressions of the moduli can be inferred.

*$\beta$ functionality of the error.* As already discussed by Tassieri *et al.*,[8] the oversampling factor $\beta$ plays a crucial role up to a value of $\beta \approx 10^3$, above which no significant improvements of the outcomes are observed, while the computational performance of the personal computer starts to be affected. In what follows, a value of $\beta \simeq 10^3$ has been used for all the data analysis, unless specified otherwise within the text.

*$T_a$ functionality of the error.* In Figure 2 we report the MRAE of the viscoelastic moduli evaluated by means of i-Rheo ***GT*** in the case of a simple Maxwell fluid with a characteristic relaxation time $\tau$ varying from $10^{-5}$ sec to $10^5$ sec across an observation time window of $[0.01, 100]$; which implies $T_a \in [-0.75, 1.75]$. From Figure 2, it is possible to identify three

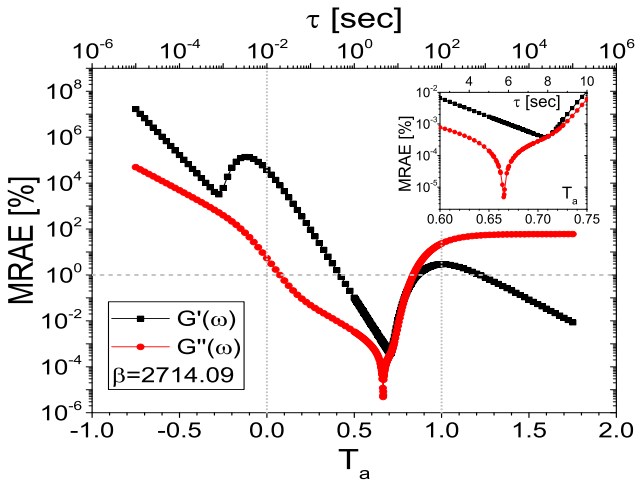


Figure 2: The Mean-Relative-Absolute-Error (MRAE) *vs.* $T_a$ of the viscoelastic moduli evaluated by means of i-Rheo ***GT*** in the case of a simple Maxwell fluid. The fluid's characteristic relaxation time $\tau$ (top axis) is varying across the observation time window $[0.01, 100]$, which is outlined by the dot lines. The dash line is a guide for the eye to MRAE $= 1\%$. The inset highlights the minima in the MRAE of both the moduli.

characteristic regions: (i) for $T_a < 0$ the fluid relaxes faster than the shortest observation time (i.e., $\tau < t_1$; a circumstance that is not always predictable) and no useful information can be gained from the measurement. In this region, both the MRAEs rapidly decreases as $T_a$ approaches the zero value from the left; with a yet unclear non-monotnic behaviour in the case of the elastic modulus. (ii) For $0 < T_a < 1$ the fluid's characteristic relaxation time falls within the observation time window and the viscoelastic properties can be retrieved to a 'certain' accuracy depending on $T_a$. In particular, it is possible to determine the fluid's viscoelastic properties to a relatively high precision (i.e., MRAE $< 1\%$) for $T_a \in [0.42, 0.82]$; where the viscous and the elastic moduli show the existence of minimum MRAE values at $T_a \cong 0.66$ and $T_a \cong 0.70$, respectively (see inset of Figure 2). (iii) For $T_a > 1$ the fluid relaxes slower than the upper limit of the experimental time window (i.e., $\tau > t_N$) and its dynamics asymptotically resemble those of a purely elastic solid as $\tau$ tends to $+\infty$. In this case, the MRAE of the viscous modulus tends to a constant value of $\cong 60\%$; whereas, the MRAE of the elastic modulus keeps decreasing (almost exponentially MRAE $\propto e^{-T_a}$) from a starting value of $\cong 3\%$ at $T_a = 1$.

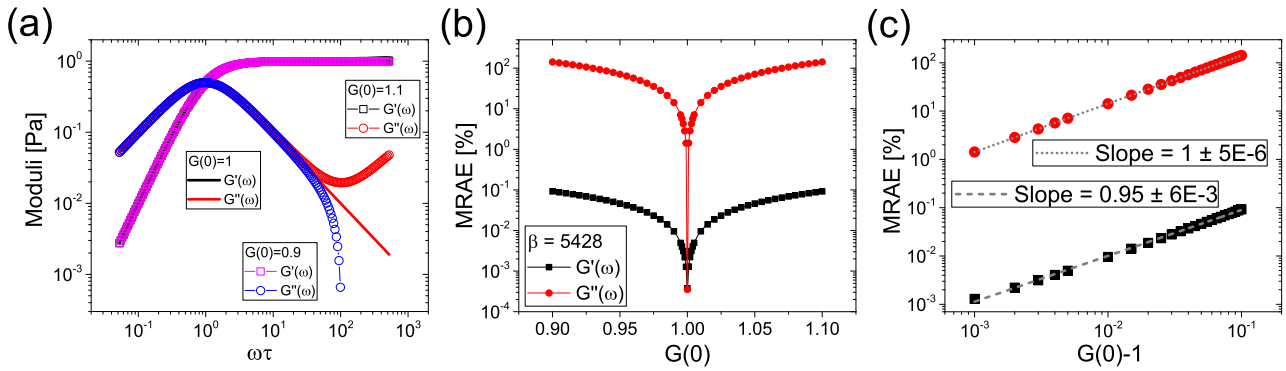


Figure 3: (A) The viscoelastic moduli derived by means of i-Rheo ***GT*** for three values of $G(0)$: $0.9, 1, 1.1$, respectively, of a single mode Maxwell fluid with $\tau = 5.25$ sec that corresponds to $T_a = 0.68$ for an observation time window of $[0.01, 100]$. (B) Mean-Relative-Absolute-Error (MRAE) of both the moduli as function of $G(0) \in [0.9, 1.1]$ for the same Maxwell fluid mentioned in (a). (C) The MRAE shown in (b) as function of $(G(0) - 1)$. The lines are the best linear fits of the same data as in (b), but only for $G(0) > 1$ (given the symmetry of the data).

$G(0)$ *functionality of the error.* In Figure 3 we report the behaviour of the MRAE of both the moduli as function of $G(0)$ for the case of a single mode Maxwell fluid with $\tau = 5.25$ sec, which corresponds to $T_a = 0.68$ for an observation time window of $[0.01, 100]$. The value of $G(0)$ is varied by $\pm 10\%$ around its ideal value of 1. From Figure 3a it is clear that $G''(\omega)$ is more sensitive than $G'(\omega)$, especially at high frequencies. In particular, from Figure 3b it can be seen that the MRAE of $G''(\omega)$ goes above 1% with just a $\pm 0.1\%$ variation of $G(0)$; whereas, the MRAE of $G'(\omega)$ remains below 0.1% over the explored range of $G(0)$. Notably, these results can be proven valid analytically by taking into account the first two terms on the right side of Equation 5, where $G(0)$ provides its contribution to the Fourier transform in Equation 3. Indeed, by considering Equations 3 and 5 evaluated at $\omega = 1/t_1$ one could write:

$$G^*(1/t_1) \cong G(0) - i\left(1 - e^{-i}\right)(G_1 - G(0)) \tag{12}$$

where we remind that $[t_0 = 0, G(0)]$ and $[t_1, G_1]$ are the first two points of the discrete data

set describing $G(t)$. From Equations 10, 11 and 12, for $t_1 << \tau$ it follows that:

$$RAE(G'(1/t_1)) \propto |(G(0) - 1)| \tag{13}$$

and

$$RAE(G''(1/t_1)) \propto |(G(0) - 1) \left(\frac{t_N}{t_1}\right)^{T_a}| \tag{14}$$

where $RAE(\cdots)$ indicates the Relative-Absolute-Error and it has been assumed that (i) $(1 - G_1)/t_1 \cong 1/\tau$ for a Maxwell fluid and in Equation 14 that (ii) $(\tau/t_1) = (t_N/t_1)^{T_a}$ from Equation 9. Equations 13 and 14 validate the numerical results reported in Figure 3 (and we anticipate in Figure 4, too), as the MRAE of both the moduli grow linearly with $|(G(0)-1)|$, as highlighted in Figure 3c.

Let us now investigate the frequency-dependence of the RAE of the moduli for a set of single mode Maxwell fluids ($\tau_i$), all evaluated by means of i-Rheo ***GT*** with an *erroneous* value of $G(0) = 1.1$ and over different observation time windows $[t_1, t_N]$, for which $t_N$ is kept constant at 100 sec and $t_1$ is varied as reported in the legends of Figure 4. From this, it possible to confirm that the elastic modulus is better estimated than the viscous modulus over the entire range of explored frequencies. In particular, the $RAE(G'(\omega))$ has a parabolic shape centred around $\omega\tau \simeq 1$. It starts with relatively low values at the extremes of the frequency window (in agreement with Equation 13 at high frequencies) and rapidly vanishes down to the machine's numerical resolution as $\omega\tau$ approaches the unit value. On the other hand, $RAE(G''(\omega))$ starts with relatively high values at high frequencies in agreement with Equation 14 and decreases quadratically until $\omega\tau = 1$, after which it remains constant at values that are inversely proportional to $(t_N/t_1)^{T_a}$ for $\omega\tau < 1$, as highlighted by the master curve drawn in Figure 4(d). At this point it is interesting to highlight that, while $RAE(G''(\omega))$ seems to follow specific scaling laws, $RAE(G'(\omega))$ shows a complex and *yet undefined* dependency on the systems' characteristic time scales (i.e., $[t_1, t_N, \tau]$), as shown

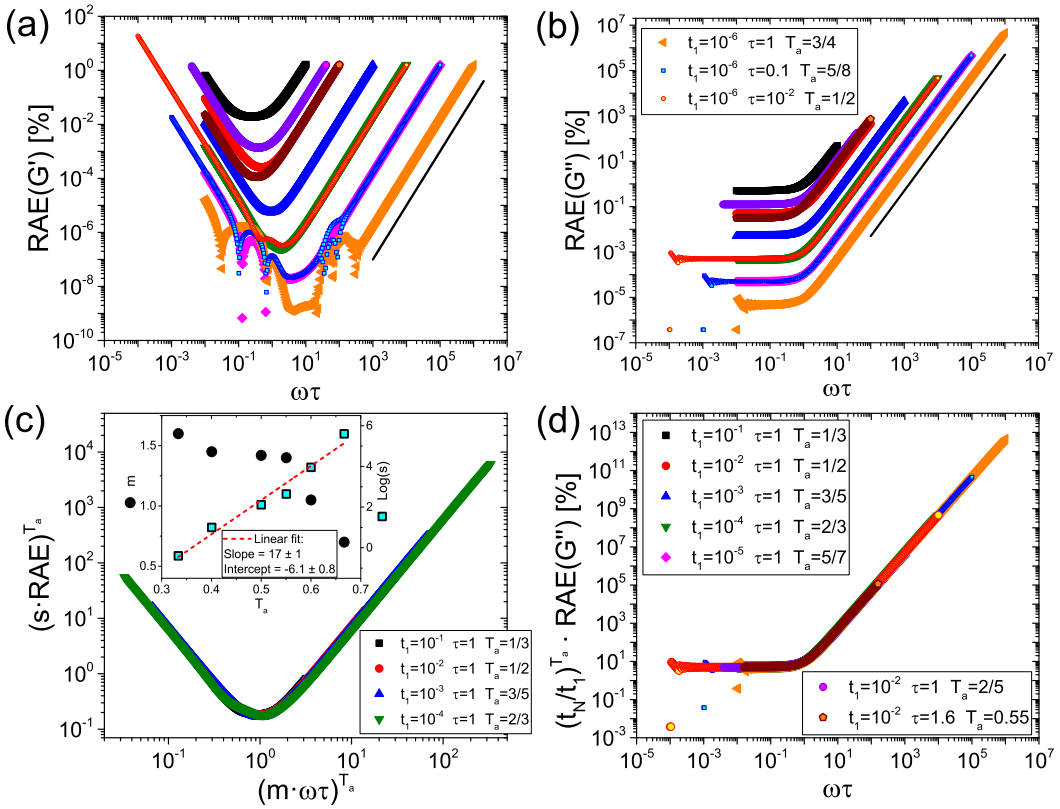


Figure 4: (a, b) The Relative-Absolute-Error (RAE) of the moduli vs. frequency of a set of single mode Maxwell fluids for different values of $T_a$, which is varied by changing either $\tau$ [sec] or the observation time windows $[t_1, t_N]$; i.e., $t_1$ [sec] is varied as reported in the legends, whereas $t_N$ is kept constant at 100 sec. All the RAE curves have been evaluated by means of i-Rheo ***GT*** with a value of $G(0) = 1.1$. The solid lines are guides for the power law $RAE \propto (\omega\tau)^2$. (c, d) Master curves of the RAE of the moduli derived from the same data shown in (a, b). The inset in (c) shows the two adjustable parameters (m,s) as function of $T_a$, they have been used to draw the master curve in (c). Notice that, data in figures (a), (b) and (d) share the same legends.

in Figure 4(c) and by the inset therein, where the parameters (m,s) used for building the master curve drawn in the main graph have been plotted against $T_a$.

Confident of the effectiveness of i-Rheo ***GT*** in educing the frequency-dependent material's linear viscoelastic properties from the analysis of the time-dependent $G(t)$, we have adopted it to analyse the dynamics of polymeric systems by means of molecular dynamics simulations based on both coarse-grained and atomistic models; as described in the following two sections, respectively.

## 3.2 Coarse-grained approaches

To overcome computational difficulties due to the long time nature of relaxation behaviors of polymeric systems, many theoretical attempts have been made to develop coarse-grained models, such those described in Ref.[26,27] A common feature of these approaches is that the polymer chain is replaced by a simplified molecular model made of freely jointed springs, and the chemistry details of molecules are embedded into a few model parameters. This simplification is based on the experimental evidences of the universality of the statistics and dynamics of polymeric systems.[2] Nevertheless, owing to the great reduction of the systems' degrees of freedom due to the coarse-graining process, analytical expressions for their rheological characterisation can be derived in the case of 'simple' systems. This is indeed the case for the pioneering molecular models proposed by Rouse,[28] Zimm,[29] and Doi-Edwards,[30] for which $G(t)$ is formulated as the sum of weighted exponential decay functions, and for which the analytical expressions of $G'(\omega)$ and $G''(\omega)$ are obtained straightforwardly. However, in general, simple models do not correlate always well with experimental data, especially at short time scales. In particular, for entangled polymers a few important relaxation mechanisms, namely 'contour length fluctuation'[31] and 'constraint release',[32] are usually required to be considered in addition to the underlying "*reptation*" dynamics conceived in the original Doi-Edwards model.[33] Therefore, the continuous increase of the number of additional molecular mechanisms, aimed at better describing the polymer systems dynamics, has made almost prohibitive the attainment of simple analytical expressions of $G(t)$; hence, the development of stochastic simulations to provide a numerical solution to the problems that otherwise would remain undetermined. In stochastic simulations $G(t)$ is obtained from the auto-correlation function of stress, as for the molecular dynamics simulations explained in the previous section; then a numerical conversion of $G(t)$ to $G'(\omega)$ and $G''(\omega)$ is necessary to compare the simulation results with the experiments. At this point it is important to remind that, due to the coarse-grained nature of the adopted models, the short-time (i.e., high-frequency) behaviour of $G(t)$ is smeared out, and therefore the simulation data in this

regime must be discarded.

In the following subsections two different stochastic simulation methods[34,35] are introduced and their effectiveness is corroborated by means of a direct comparison between experimental bulk rheology data and those obtained from the transformation of $G(t)$ by means of both Reptate and i-Rheo ***GT***.

### 3.2.1 Methods

The first simulation method we wish to introduce is the so-called '*primitive chain network*' (PCN),[34] in which an entangled polymeric liquid is replaced by a network consisting of nodes, strands and dangling ends. In particular, one polymer chain corresponds to a path connecting a pair of dangling ends through the network nodes in between. At each network node, there exists a slip-link that allows the polymer chains connected at the node to slide along their contour. The sliding motion of the chain and the motional constraint induced by the slip-links along the chain are aimed at reproducing the reptation dynamics. In this model, the contour length fluctuations are also considered, and the slip-links (and the corresponding network nodes) are removed when one of the involved polymer chains slides off. On the contrary, a new slip-link is created on a dangling segment to connect it to another surrounding segment when the dangling segment becomes sufficiently large as a result of the chain sliding. The state variables of the system are the position $\{\boldsymbol{R}\}$, the number $\{Z\}$ of slip-links (network nodes) on each chain, the number of Kuhn segments on each network strand and the number of dangling segment $\{n\}$. The time dependence of $\{\boldsymbol{R}\}$ and $\{n\}$ obey to Langevin-type equations, in which different force components such as the drag force, the local tension on each segment, the osmotic force suppressing density fluctuation and the random force due to thermal agitation are considered. The time-dependent fluctuation of $\{Z\}$ is induced by the creation/destruction of slip-links at the chain ends as mentioned above. Actually, for the removal and creation of slip-link at the chain end, the number of Kuhn segments on the outmost entanglement segment is observed.[34,36] For a deeper understanding of the principles

underpinning this simulation scheme, we refer the reader to Ref.[26,34] and those therein.

The second simulation method is the '*multi-chain slip-spring*' (MCSS).[35,37–40] In this case, a number of Rouse chains connected by the virtual springs are dispersed in a simulation box. These springs mimic the entanglements between chains by restricting the chain dynamics. Namely, the virtual springs are allowed to slide along the chain contour and to be created/destructed at the chain ends. Owing to the tracing for the Rouse beads between entanglements, MCSS simulations can reproduce the chain dynamics in the frequency domain that is in between those explored by microscopic simulations and those investigated by PCN simulations.

### 3.2.2 Results

In this section, we compare bulk-rheology measurements with the results obtained from i-Rheo ***GT*** and Reptate on the numerical conversion of $G(t)$ to $G^*(\omega)$ for both the cases of PCN and MCSS simulations. Reptate is a software that achieves the conversion under the assumption that $G(t)$ can be represented by a linear combination of single exponential decay functions. Due to the ill-posed nature of the fitting for such functions, the conversion result from Reptate depends on the initial guess of the fitting parameters, i.e. the relaxation intensity and the relaxation time of each mode. In particular, the fitting procedure at short-time scales of $G(t)$ is not straightforward and a criterion or guide is necessary. In the results shown in this section, the parameters choice in Reptate was made to recover the numerical conversion by the method proposed by Schwarzl.[41]

Let us start by corroborating the concepts introduced in Section 3.1 for the ideal cases of single mode Maxwell fluids when these are applied to real polymeric systems. In particular, in Figure 5 are drawn together the linear bulk-rheology measurements of three highly monodisperse polyisoprene melts and their respective relaxation moduli, $G(t)$, obtained by means of PCN simulations[43] (Figure 5(a)) and Fourier transformed either via Reptate or i-Rheo ***GT***. Notably, thanks to their high monodispersity, it is actually possible to define a $T_a$

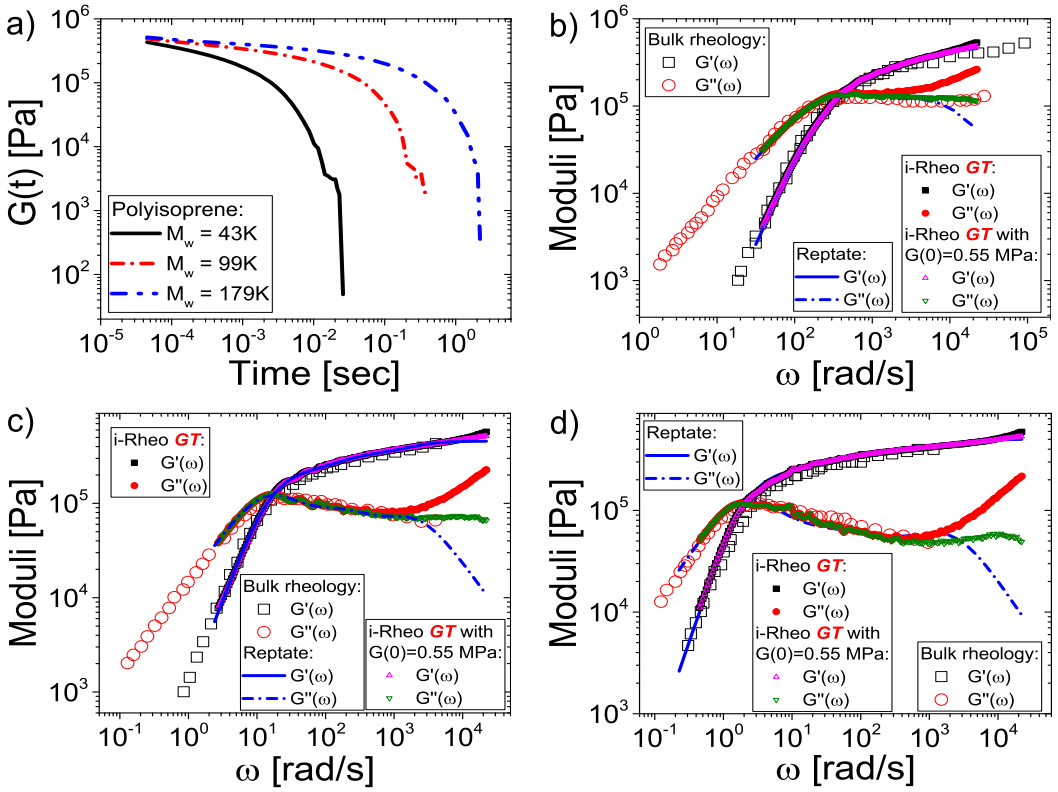


Figure 5: Comparison between the linear bulk-rheology measurements of highly monodisperse polyisoprene melts (b) $Mw = 43$k, (c) $Mw = 99$k, (d) $Mw = 179$k and their viscoelastic properties educed from PCN simulations of $G(t)$ (a) converted by means of both Reptate (with fourteen modes) and i-Rheo ***GT***. The bulk-rheology data have been taken from Ref.[42,43]

value for each system reported in Figure 5. This is achieved by means of their bulk-rheology measurements, i.e. by using the abscissa of the moduli's low-frequency crossover as a measure of the material's characteristic time. Therefore, one could calculate: (b) $T_a \cong 0.65$, (c) $T_a \cong 0.79$ and (d) $T_a \cong 0.83$, all very close to the optimum values of $T_a \cong 0.66$ and $T_a \cong 0.70$ reported in Figure 2; preluding good outcomes from the transformation of MD simulations.

From Figure 5 it is clear that both the analytical tools perform equally well, showing good agreement with experimental data almost over the entire range of frequencies. However, it is important to highlight that at very high frequencies, they both seem to provide slightly diverging values of the moduli. In particular, while $G'(\omega)$ shows good adherence to the frequency-behaviour of the bulk data, with very subtle differences between the methods;

$G''(\omega)$ shunts significantly from the expected values, for all three systems. This is mainly due to the (erroneous) value of $G(0)$ assumed during the transformation process of $G(t)$ performed by the two analytical tools; here returning similar results to those shown in Figure 3a. In the case of Reptate, the fitting procedure works on the logarithm values of both $G(t)$ and $t$, therefore discarding the original value of $G(0)$ at time $t = 0$ (for obvious reasons) and replacing it with a lower one obtained from the fastest Maxwell mode ($G_1$) of Equation 4. This leads to lower values of $G''(\omega)$ at high frequencies, as for the case of the single mode Maxwell fluid reported in Figure 3a with $G(0) = 0.9$. In the case of i-Rheo ***GT***, the up-turn of $G''(\omega)$ is mainly due to the lack of information on the temporal behaviour of $G(t)$ within the time window $]0, t_1[$, in which the analytical tool interpret the missing data by means of a numerical interpolation between those two points. This is very similar to the case of the single mode Maxwell fluid shown in Figure 3a with $G(0) = 1.1$. Nevertheless, when needed like in this case, i-Rheo ***GT*** offers the opportunity of a better interpretation of the experimental data by tuning the initial parameter $G(0)$. Indeed, it can be seen that by changing the original value of $G(0) = 0.9$ MPa to $G(0) = 0.55$ MPa, a better agreement is achieved between the bulk-rheology data and those obtained from MD simulations, for all three systems. Interestingly, this value is very close to the *unit modulus* $G_0 = 0.6$ MPa reported by Masubuchi *et al.*[43]

Figure 6 shows a comparison between the bulk-rheology measurements of a polystyrene melt ($Mw = 96.4$k, taken from Ref.[40]) and those educed from MCSS simulations of $G(t)$ (see inset) transformed by means of both Reptate and i-Rheo ***GT***. Also in this case, it can be seen that, at low frequencies both the analytical tools show a good agreement with the experimental data; whereas, at high frequencies, it seems that Reptate provides a closer agreement than i-Rheo ***GT***. However, it is important to highlight that, despite such discrepancy, the frequency behaviour of the moduli evaluated by means of i-Rheo ***GT*** better resemble those of bulk-rheology measurements, especially in the case of $G''(\omega)$. Interestingly, this feature will be addressed and fully elucidated in the following section; but we anticipate that (as

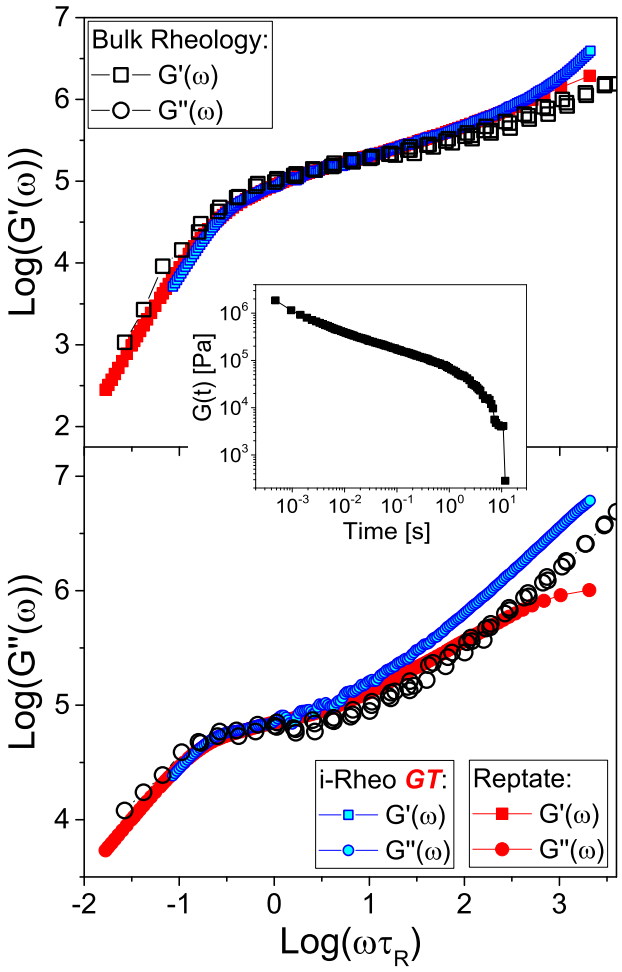


Figure 6: Comparison between the linear bulk viscoelastic properties of a polystyrene melt ($Mw$ = 96.4k) and those educed from a MCSS simulation of $G(t)$ (see inset) transformed by means of both Reptate (with six modes) and i-Rheo ***GT***. The bulk-rheology data have been taken from Ref.[40]

for the systems shown in Figure 5) it is directly related to both the finite range of explored dynamics (owing to the inherent limited time window explored by coarse-grained simulation methods) and to the use of a generalised Maxwell model to perform the Fourier transform of $G(t)$ in the case of Reptate. We recon that such a critical investigation is necessary for further understanding and improvements of theoretical models.

## A molecular approach

In the following sections, two case studies that use i-Rheo ***GT*** to analyse the results of molecular dynamics simulations are presented. In both cases, the relaxation modulus was calculated on the fly during the simulations. The calculated relaxation modulus was then transformed into the complex modulus. The accuracy of the obtained viscoelastic moduli and the advantages of using i-Rheo ***GT*** for the conversion are discussed.

## 3.3 Coarse-grained Langevin simulations of entangled polymers

### 3.3.1 Methods

In this section, we focus on dense polymer liquids by modelling the polymers as bead-spring chains with no intrinsic stiffness.[44] In this model, the chain monomeric units are represented as spheres of diameter $\sigma$ and mass $m$. All monomeric units interact via a purely repulsive Lennard-Jones (LJ) potential (excluded volume interaction),

$$U_{LJ}(r) = \begin{cases} 4\epsilon \left[ \left(\frac{\sigma}{r}\right)^{12} - \left(\frac{\sigma}{r}\right)^{6} + \frac{1}{4} \right] & \text{for} \quad r < r_c \\ 0 & \text{for} \quad r \geq r_c \end{cases} \tag{15}$$

where $\epsilon$ is the energy scale of the potential, $r$ is the distance between two interacting monomers and $r_c = 2^{1/6}\sigma$ is the cutoff distance for the potential. The polymers are formed by connecting the monomers with an additional finitely extensible nonlinear elastic (FENE) spring potential defined as

$$U_{FENE} = -(kR_0^2/2)\ \log(1 - r^2/R_0^2), \tag{16}$$

where $k$ is the spring constant of the bond and $R_0$ is the maximum allowed extension of the finitely extensible bond between two beads. The equations of motion are integrated using the Verlet algorithm, in which all monomers are weakly coupled to a Langevin heat bath with coupling of $\Gamma = 0.5/\tau_{LJ}$ at a temperature of $T = \epsilon/k_B$;[44] where $\tau_{LJ} = \sigma(m/\epsilon)^{1/2}$.

The time step for the integration is $\Delta t = 0.012\tau_{LJ}$. For the spring potential, we have used $k = 30\epsilon/\sigma^2$ and $R_0 = 1.5\sigma$.[45] The parameter choice yields an average bond length $b \approx 0.97\sigma$ and guarantees sufficiently close contact between connected monomers to prevent chain crossings.

Using the model described above, monodisperse polymer melts of $50-100$ chains of length $40 \leq N \leq 350$ at a bead density of $\rho = 0.85\sigma^{-3}$ were simulated.[7,46] Even in the absence of any intrinsic stiffness, these polymer chains are non-Gaussian at short length scales and the mean square internal distances are proportional to $(N-1)$ only for $N \gtrsim 100$. For such chain lengths, the $c_\infty b^2 \equiv \langle R^2 \rangle/(N-1) = 1.75\sigma^2$.[45] Here, $c_\infty$ is the Flory characteristic ratio, $b$ is the average bond length, $\langle R^2 \rangle$ is the mean-square end-to-end distance of the chain and $N$ is the number of monomers in the chain. As described in more detail in Ref.,[7,46] the time-dependent shear relaxation modulus for all the systems mentioned above were calculated and have been here reanalysed as discussed below.

### 3.3.2 Results

Likhtman *et al*[7] converted the $G(t)$ calculated using MD simulations by means of a generalised Maxwell model. The resulting frequency-dependent viscoelastic moduli led them to opine that the Kremer-Grest model for entangled polymer liquids was undermined by the following issue:

"*The only qualitative disagreement is that the* $G'(\omega)$ *and* $G''(\omega)$ *obtained from MD do not cross around* $\tau_e$*, but are approximately parallel to each other for* $\omega > 1/\tau_e$*. In contrast to that, the experimental melt data always have* $G''(\omega) > G'(\omega)$ *at high frequency....where* $G''(\omega)$ *always crosses* $G'(\omega)$ *and exceeds it by a factor of* 2 *or so at higher frequency*" (see Figure 4 in Likhtman *et al.*[7]).

We can now assert that the finding that led to the above opinion was misleading and arose because of the preconceptions inherent in the analytical method adopted by Likhtman *et al.*[7] to transform the $G(t)$ to $G^*(\omega)$; i.e., a generalised Maxwell model (see Equation 4). Now

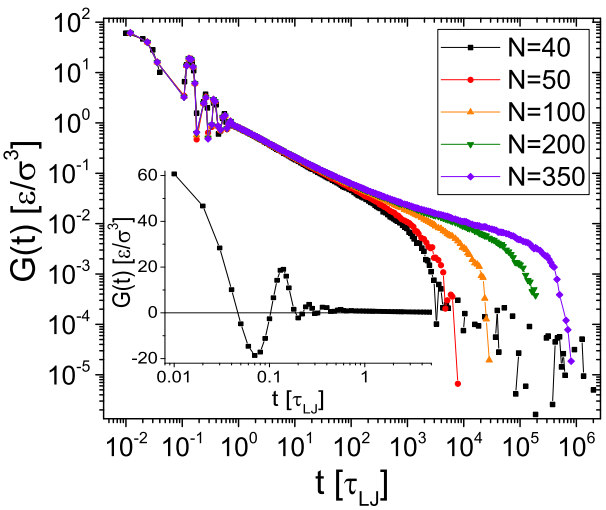


Figure 7: Stress relaxation for the standard Kremer and Grest[44] polymer model with molecular weights of $N = 40, 50, 100, 200$ and 350. The inset highlights the short time oscillating behaviour of $G(t)$ for N=40. Data taken from Likhtman *et al.*[7]

that we have the '*right tool*' to convert $G(t)$ to $G'(\omega)$ and $G''(\omega)$, the qualitative discrepancy with experimental data accentuated by Likhtman *et al.*[7] disappears.

In Figure 7 we revisit a selection of stress relaxation curves originally presented by Likhtman *et al.*[7,46] The inset highlights the short-time oscillations of $G(t)$, which are due to the underdamped vibrations of the bonds connecting the beads in the adopted model. These fluctuations are typically discarded, partly due to the absence of an effective analytical method for data analysis such as the one introduced here.

In Figure 8 we report the viscoelastic moduli of two monodisperse polymer melts with $N = 40$ (unentangled) and $N = 350$ (entangled) obtained by converting the $G(t)$ shown in Figure 7 using i-Rheo ***GT*** with a value of $G(0) = 66.1\ \epsilon/\sigma^3$ for both the systems. The results clearly show the existence of a high frequency crossover in the moduli at $\omega_{cross} \cong 1.49 \times 10^{-3}\tau_{LJ}^{-1}$ for $N = 350$. This establishes that the high frequency discrepancy between the Kremer-Grest model and the experimental data highlighted by Likhtman *et al.*[7] can be ascribed to an artefact of their procedure to convert $G(t)$ into $G'(\omega)$ and $G''(\omega)$. This will be discussed further in the next section. Moreover, the inset of Figure 8 confirms the theoretical expectation of $tan(\delta(\omega)) \simeq 2$ for $\omega\tau_e > 10$; here, with a maximum value of $tan(\delta(\omega)) \cong 3$

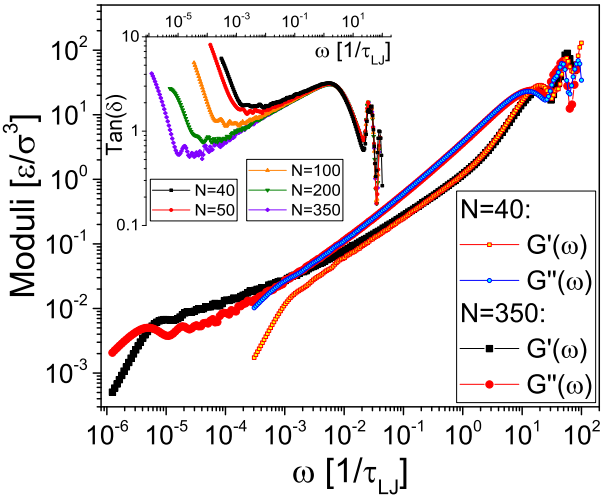


Figure 8: The viscoelastic moduli of two monodisperse linear polymers with $N = 40$ and $N = 350$ evaluated by feeding the respective *raw* data of $G(t)$ shown in Figure 7 into i-Rheo ***GT***, and both transformed by using a $G(0)$ value of 66.1 $\epsilon/\sigma^3$. The inset shows the frequency behaviour of $tan(\delta)$ for all the systems reported in Figure 7.

at $\omega\tau_e \simeq 10^3$, assuming $\tau_e \simeq 1/\omega_{cross} \simeq 671$. Interestingly, this value is smaller than those reported in literature of $\tau_e \approx 5800$ by Likhtman *et al.*[7] (which was obtained by fitting the relaxation modulus with a single-chain slip-spring model) and of $\tau_e \approx 2950$ by Wang *et al.*[47] (which was obtained from the mean-square displacement of the middle monomer); these values were both estimated from simulations based on the same flexible KG polymer model. Notice that, as elucidated in Section 3.1, in this case a $\pm 10\%$ variation of $G(0)$ would only affect the evaluation of $\omega_{cross}$ by less than $\pm 2\%$, with corresponding values of $\tau_e \in [662, 685]$.

The results reported in Figure 8 prove that i-Rheo ***GT*** is a valuable new rheological tool capable of extending the analysis of rheological data all the way up to the materials' glassy modes and even beyond. At the short time scales, MD simulations are likely to provide the most statistically accurate values of $G(t)$. However, existing algorithms struggle to accurately convert these data into the frequency domain and therefore do not assist in their interpretation. This is further explored and confirmed in the following section.

The above analysis also allows us to affirm that the viscoelastic moduli calculated using the Kremer-Grest model are indeed qualitatively consistent with experimental data even at high frequencies. In addition, for the accurate calculation of the stress relaxation (and the

mean-square displacements), at negligible additional computational cost, during simulations of the Kremer-Grest model over a wide range of chain lengths, densities, temperatures, and chain stiffnesses, we can endorse both the theoretical method and the software correlator based approach introduced by Likhtman *et al.*[7]

## 3.4 Atomistic MD simulations of polyethylene

### 3.4.1 Methods

A series of MD simulations of linear monodisperse polyethylene chains of different molecular weights, ranging from 0.34 to 14 kDa (roughly 0.5 to 18 entanglements), have been run. A united-atom approach has been adopted, in which carbon atoms and their bonded hydrogens are merged into single, spherical interaction sites. Distinction is made between methylene ($CH_2$) and methyl ($CH_3$) units with respect to non-bonded interactions, but not for the bonded ones. Bond lengths and angles are subject to harmonic potentials given by:[48]

$$U_{bond} = k_B k_l (l - l_0)^2/2 \tag{17}$$

$$U_{bending} = k_B k_\theta (\theta - \theta_0)^2/2 \tag{18}$$

where $k_l = 96500\ \mathrm{K} \cdot \mathrm{\AA}^{-2}$ and $k_\theta = 62500\ \mathrm{K} \cdot \mathrm{rad}^{-2}$. The equilibrium bond length and bending angles are $l_0 = 1.54$ Å and $\theta_0 = 114°$, respectively. Rotations around bonds are governed by the 9-term Toxvaerd torsional potential.[49] Interactions between pairs of sites that belong to different molecules and pairs on the same molecule that are separated by at least 4 bonds are described by a standard $12-6$ Lennard-Jones potential:

$$U_{LJ} = 4\epsilon_{ij}\left(\left(\frac{\sigma_{ij}}{r_{ij}}\right)^{12} - \left(\frac{\sigma_{ij}}{r_{ij}}\right)^{6}\right) \tag{19}$$

where the values of the interaction parameters, $\sigma_{CH_3} = 3.91$ Å, $\sigma_{CH_2} = 3.95$ Å, $\epsilon_{CH_3}/k_B = 104$ K and $\epsilon_{CH_2}/k_B = 46$ K, have been taken from the TraPPE potential.[50] The standard

Lorentz-Berthelot mixing rules have been used for the interaction parameters between $CH_3$ and $CH_2$ units. A cut-off of 9 Å has been used for the calculation of non-bonded interactions and a long-range tail correction for the energy and pressure has been used.

All simulations have been conducted under periodic boundary conditions in all dimensions. All systems have been previously equilibrated through extensive Monte Carlo (MC) simulations based on the double bridging (DB) and intramolecular double rebridging algorithms.[51,52] MC simulations have been executed in the NPT ensemble, at 1 atm and 450 K producing thousands of uncorrelated and equilibrated system configurations. After the equilibration step, computer-generated polymer configurations, representative of system's average chain size and density have been selected for long MD simulations in the NVT ensemble, at 450 K and at the constant volume as obtained in the MC simulations. Temperature has been kept constant by means of a Nose-Hoover[53,54] thermostat, with a damping parameter $T_{damp} = 100$ fs. The rRESPA multiple time step algorithm[55] has been used for the integration of the equations of motion, with 1 fs and 5 fs as short and long time steps, respectively. All MD simulations have been run using a modified version of the LAMMPS software[56] in parallel executions, using from 16 up to 128 CPUs. Atomic velocities and coordinates along with thermodynamic information have been recorded every 5 ps for all systems except for the $C_{500}$ and the $C_{1000}$ ones; for which frames have been stored every 10 ps for a total MD simulation time exceeding 15 $\mu$s.

### 3.4.2 Results

Figure 9 shows the relaxation modulus of the samples ranging from 0.34 to 14 kg/mol. At early times, $G(t)$ shows large oscillations due to bonded interactions. These oscillations are independent by the molecular weight, last up to $10^{-3}$ ns and cause the modulus to become negative before decaying to zero. After they die out, a combination of Rouse relaxation (with $G(t) \propto t^{-0.5}$) and glassy modes can be observed. Then, the modulus of unentangled samples (with $M_w \lesssim 1$ kg/mol) decays exponentially, whereas entangled samples show the existence

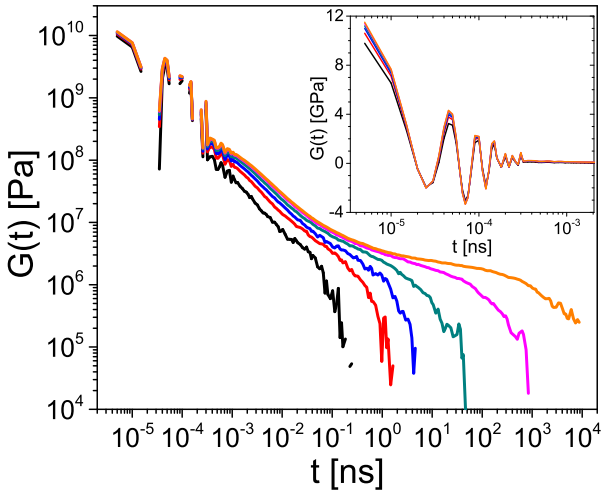


Figure 9: Relaxation modulus of atomistic simulations of monodisperse linear polyethylene with molecular weights (left to right) $N = 24, 48, 78, 142, 400$ and 1000 carbon atoms (corresponding to $0.34, 0.67, 1.09, 1.99, 5.6$ and 14 kg/mol, respectively). The inset shows the short time oscillating behaviour of $G(t)$.

of a rubbery plateau that also decays exponentially, but at longer times. The time step is of the order of 1 fs, which is $5-6$ decades smaller than the time at which entanglement effects are initially felt by the linear polymers. This limits the range of time over which we can investigate entanglement dynamics, because the practical limit of realistic MD simulations is of the order of $10^8 - 10^9$ time steps. In addition, the value of the plateau modulus is $3-4$ decades lower than the amplitude of the relaxation modulus due to intramolecular stress oscillations. In order to obtain an accurate value of the plateau modulus and the stress relaxation in the terminal region, a very high signal to noise ratio is needed, which requires to calculate the stress autocorrelation function as frequently as possible. This is possible with the help of the correlator algorithm[20] described in Section 2.3, which has been implemented as a *fix* (named ave/correlate/long) in the LAMMPS software.

We now wish to demonstrate the advantages gained by using i-Rheo ***GT*** for the conversion of $G(t)$ into $G^*(\omega)$. In order to do this, we focus the attention on one of the entangled samples shown in Figure 9; i.e., the polymer chain with $M_w = 5.6$ kg/mol. In Figure 10 are compared the viscoelastic moduli of this sample obtained by transforming its $G(t)$ both via Reptate (using a series of 20 Maxwell modes equally distant in logarithmic scale) and

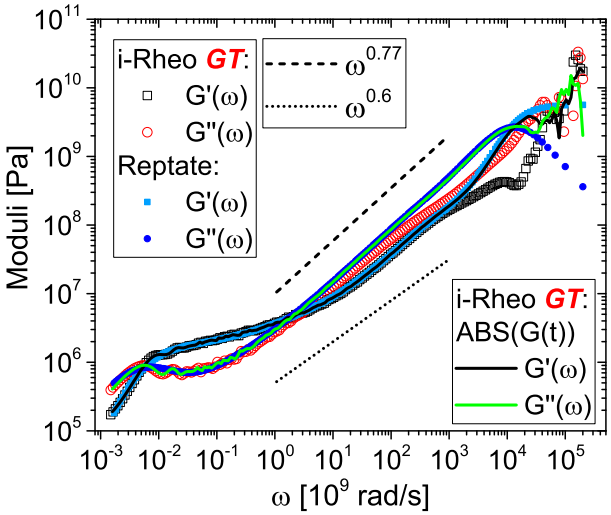


Figure 10: Complex modulus from Molecular Dynamics simulations of a monodisperse linear polyethylene sample of $M_w = 5.6$ kg/mol, as obtained by fitting a series of 20 Maxwell modes to $G(t)$ in Reptate (filled symbles) and using i-Rheo ***GT*** (open symbols), with $G(0) = 12.9$ GPa. The continuous lines represent the viscoelastic moduli obtained by transforming the absolute value of $G(t)$ with i-Rheo ***GT***. The dashed and dot lines are guides for the power laws.

i-Rheo ***GT*** (open symbols). Overall, the agreement is excellent between the two methods in the range of frequencies from $10^{-3}$ to 1 rad/ns. It should be noted that the apparent smoothness of the Reptate fitting is somehow artificial and results from the smooth character of the Maxwell fitting functions.

At higher frequencies ($\omega \gtrsim 1$ rad/ns), there is a clear discrepancy between the outcomes of the two analytical *tools*, which is highlighted by the higher power law of $G''(\omega)$ at frequencies higher than $\tau_e^{-1}$ obtained from Reptate. We must remind that, in this region (i.e., the so-called rubber-to-glass-transition zone), the material dynamics are governed by the coexistence of Rouse modes and the tail of glassy relaxation modes.[17,18] Therefore a more accurate Fourier transform of the data could potentially help to discern the relative weight of the different contributions. Moreover, it is worth to highlight that, such disparity between the outcomes starts at frequencies of the order of $1/\tau_e$; this being an important rheological parameter whose evaluation is therefore affected by the choice of the analytical method adopted to transform $G(t)$, as further discussed later on. In addition, at very high frequen-

cies ($\omega \approx 10^4$ rad/ns), the viscoelastic moduli from Reptate show a Maxwell-like behaviour, which is much simpler than the actual relaxation process shown by $G(t)$ at early times.

In order to understand the dissimilarities between the results reported in Figure 10, it should be reminded that, due to the wideness of the time window explored by atomistic MD simulations (i.e., up to 9 decades, see Figure 9), the Maxwell mode fitting procedure performed in Reptate uses the logarithm of $G(t)$, effectively discarding the negative values of the relaxation modulus observed at early time (see inset of Figure 9). We should stress that these high frequency oscillations are not artifacts of simulations. They are due to the damped vibrations of the bonded interactions in the atomistic force field and the inertia term present in the atomistic model; therefore they should not be mistreated. Notably, when the absolute value of $G(t)$ is fed to i-Rheo ***GT*** a much better agreement is obtained over the entire frequency spectrum (see Figure 10). Nevertheless, in order to obtain veracious viscoelastic moduli, we believe that atomistic MD simulation data at early times should not be discarded nor misused, as they carry the most statistically valid predictions of $G(t)$. However, due to the inherent difficulty of fitting a small number of Maxwell modes to the highly oscillating shape of the relaxation modulus, we strongly support the use of an accurate Fourier transform method like the one implemented in i-Rheo ***GT***.

The advantages of using i-Rheo ***GT*** become apparent when the systems' characteristic relaxation times are extracted from atomistic MD simulation data, as reported in Figure 11(a). In particular, according to the tube theory[3] linear chains should show three clear relaxation regimes bounded by the following characteristic times: $\tau_e$ (the Rouse time of one entanglement, obtained from the high frequency crossover of $G'(\omega)$ and $G''(\omega)$), $\tau_R$ (the Rouse time of the chain, obtained from the minimum of $\tan(\delta)$) and $\tau_d$ (the disengagement or reptation time, obtained from the low frequency crossover of the moduli). In the case of well entangled polymer systems, the value of $\tau_d$ can be determined accurately only at a very high computational cost, because simulations need to be run for times much longer than $\tau_d$. From Figure 11(a), it can be seen that: $\tau_d \propto M_w^{3.16}$, which is in very good agreement with the tube

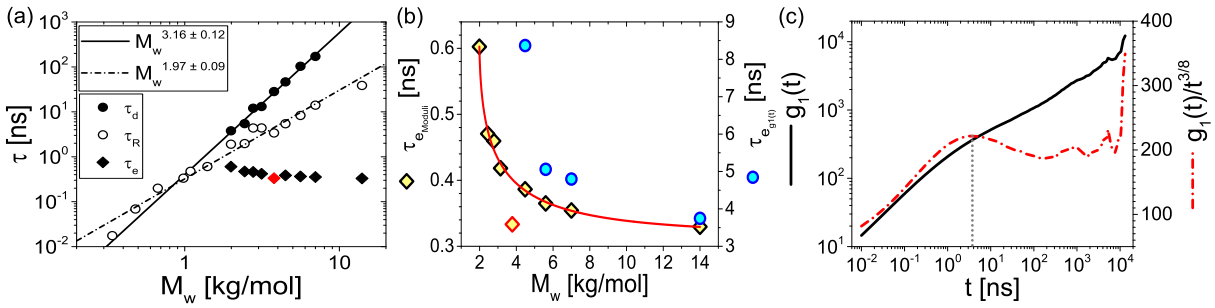


Figure 11: (a) The characteristic times $\tau_e$, $\tau_R$ and $\tau_d$ *vs.* molecular weight of monodisperse linear polyethylene melts. The characteristic times have been determined by means of the polymers' viscoelastic moduli obtained via i-Rheo ***GT*** as explained in the text. (b) The molecular weight dependence of $\tau_e$ evaluated either from the high frequency crossover of the moduli (left axis) or via the middle monomer mean-square-displacement (right axis). (c) An example of the middle monomer mean-square-displacement $g_1(t)$ of a linear polyethylene chain having $M_w = 14$ kg/mol (left axis). The same data are also shown scaled by $t^{3/8}$ (right axis). The dotted line indicates the position of a local maximum of the function $g_1(t)/t^{3/8}$, whose abscissa provides a reading of $\tau_e$ (reported in (b), right axis) as elucidated in the body of the manuscript.

theory predictions of $\tau_d \propto M_w^3$ in pure reptation or $\tau_d \propto M_w^{3.4}$ if contour length fluctuations are taken into account; $\tau_R \propto M_w^{1.97}$, which is very close to the expected scaling for the Rouse time of $\tau_R \propto M_w^2$. With regards to $\tau_e$ (see Figure 11(b)), it is interesting to highlight that, (except for a single value) data show *for the first time* in literature a good adherence to a stretched exponential decay function (i.e., Eq. 20), which was impossible to capture before by means of other analytical tools (including Reptate). This is because the relative position of $1/\tau_e$ results to be strongly affected by the accuracy of the fitting procedure at early times, the number of Maxwell modes and by the size of the time window in which the fitting procedure is computed. To corroborate our observation, we have also estimated the value of $\tau_e$ from the mean-square-displacement of the middle monomers of the chain, $g_1(t)$ (see Fig. 11(c)); which, in compliance to the tube theory, is expected to show the following scaling laws: $g_1(t \leq \tau_e) \propto t^{0.5}$ (Rouse scaling) and $g_1(\tau_e \leq t \leq \tau_R) \propto t^{0.25}$ (Rouse scaling along a random walk). Therefore, $\tau_e$ can be estimated as the crossover time between the two regimes.[7,47] However, the transition from one dynamic scaling regime to the other is not easily identifiable as reported in Ref.[57] Nevertheless, we have estimated $\tau_e$ from the abscissa of the local

maximum of $g_1(t)/t^{3/8}$; where $t^{3/8}$ is a rationally chosen intermediate power law between $t^{0.25}$ and $t^{0.5}$ for identifying the transition between those two regimes. For chains shorter than 4.48 kg/mol, the plots of $g_1(t)/t^{3/8}$ did not show a local maximum and no values of $\tau_e$ were estimated. Whereas, for $M_w \geq 4.48$ kg/mol, the $\tau_e$ values obtained from the mean-square-displacement of the middle monomers show a similar behaviour to those obtained from the high frequency cross-over of $G^*(\omega)$ when drawn agains $M_w$ (see Figure 11(b)). (We anticipate that, a more detailed analysis of the viscoelastic and diffusion properties of the atomistic simulations reported in this section will be discussed in a forthcoming paper.) It is worth noting that, despite the $\tau_e$ values obtained from $g_1(t)$ are circa an order of magnitude higher than those evaluated from the high-frequency crossover of the moduli, such disparity (due to the adoption of different observables) is consistent with the results reported in Section 3.3.2 for the Kremer-Grest model systems (i.e., $\tau_e \simeq 671\ \tau_{LJ}$), when these are compared with the $\tau_e$ values obtained from either fitting a single-chain slip-spring model to the relaxation modulus ($\tau_e \approx 5800\ \tau_{LJ}$)[7] or via the analysis of $g_1(t)$ ($\tau_e \approx 2950\ \tau_{LJ}$).[47]

For highly entangled polymer systems (i.e., $Z \gg 1$), $\tau_e$ is expected to be independent by the polymers' molecular weight and equal to $N_e^2\zeta b^2/3\pi^2 k_B T$; where $N_e$ is the number of monomers per entanglement, $\zeta$ is the monomeric friction factor and $b$ is the Kuhn length.[58] Nevertheless, we now wish to speculate on the possible veraciousness of the newly discovered functionality of $\tau_e$, as $M_w$ approaches (from the right) the system's entanglement molecular weight value ($M_e$). Indeed, it is reasonable to argue that, lower molecular weights should have a higher free volume, due to the higher fraction of chain ends, and therefore a lower friction factor, but also a slightly higher $N_e$. Therefore, it is possible to hypothesise that the combination of all these factors may lead to a nontrivial functionality of $\tau_e$ with respect to $M_w$, like the following function used to fit the data shown in Figure 11(b):

$$\tau_e = B\Big\{1 + \exp[-(M_w/A - 2)^C]\Big\}, \tag{20}$$

where,

$$\begin{cases} A = 0.99043 \pm 9 \times 10^{-5} \quad [kg/mol] \\ B = 0.317 \pm 0.002 \quad [ns] \\ C = 0.48 \pm 0.03 \end{cases}$$

Interestingly, $A$ is almost equal to the entanglement molecular weight of polyethylene $M_e \approx 1$ kg/mol[59] and in the limit of $M_w \to \infty$, $\tau_e$ tends to an asymptotic constant value of circa 0.32 ns (in agreement with the current theoretical framework). Equation 20 shows that the molecular weight $M_w$ must be larger than $2M_e$ before $\tau_e$ can be determined precisely and entanglement effects can be revealed; in agreement with the results shown in Figure 11.

# 4 Conclusions

In this article we present and validate a new *open access* executable named 'i-Rheo ***GT***', which allows the evaluation of the materials' linear viscoelastic properties from their time-dependent shear relaxation modulus over the widest range of accessible frequencies, without the need of preconceived models. Its unbiased nature has allowed us to gain *new insights* into the materials' high-frequency dynamics, where glassy modes and atomic interactions rule their rheological behaviour. Notably, these dynamic regimes (often discarded in literature) are where atomistic molecular dynamics simulations actually provide their most statistically valid prediction of the shear relaxation modulus and where existing codes struggle to *interprete* the data.

i-Rheo ***GT*** offers the opportunity to revise the outcomes of previous rheological studies where original measurements were either explained by means of theoretical models or partially discarded because of the absence of an effective tool for data analysis, as the one presented in this work. Indeed, thanks to i-Rheo ***GT*** we have corroborated the efficacy of the pioneering method introduced by Likhtman *et al.*[7] for calculating the stress relaxation

during simulations (without significant additional central processing unit cost) of a simple bead-spring model of polymer melt, which was originally thought to be unable to provide qualitative predictions of the viscoelastic moduli at relatively high-frequencies. This was a misleading outcome ascribable to the preconceived nature of the generalised Maxwell model adopted to interpret the data in the original work.

Finally, by analysing the results obtained from atomistic molecular dynamic simulations of entangled monodisperse linear polyethylene melts, i-Rheo ***GT*** allows us to identify *for the first time* in literature a stretched exponential functionality of the entanglement time with respect to the polymer molecular weight. Inferring that a constant value of the entanglement time should be expected only for highly entangled systems; i.e., for a number of entanglements exceeding a value of twenty, circa.

To conclude, i-Rheo ***GT*** represents a valuable new tool for all those theoretical and simulation studies aimed at developing/solving comprehensive models potentially able to predict the materials' linear viscoelastic properties over the widest range of experimentally accessible frequencies.

## Acknowledgement

The authors thank Mike Evans, Richard Graham, Robert Poole and Giovanni Ianniruberto for helpful conversations. JR and NCK acknowledge financial support from projects MAT-2010-15482, MAT2015-70478-P and FIS2016-78847-P of MINECO/FEDER, as well as the computer resources and technical assistance provided by the Centro de Supercomputacion y Visualizacion de Madrid (CeSViMa). SKS was supported by JSPS KAKENHI Grant Numbers JP26800221, JP15K05619 and by the Collaborative Research Program of Institute for Chemical Research, Kyoto University (Grant Number 2017-47).

# References


(1) Rapaport, D. C. *The art of molecular dynamics simulation*; Cambridge university press, 2004.

(2) Ferry, J. D. *Viscoelastic properties of polymers*, 3rd ed.; Wiley, 1980.

(3) Doi, M.; Edwards, S. *The Theory of Polymer Dynamics*; Oxford University Press, Oxford, UK, 1988.

(4) Rubinstein, M.; Colby, R. H. *Polymer Physics*; Oxford University Press: Oxford, 2003.

(5) Kmiecik, S.; Gront, D.; Kolinski, M.; Wieteska, L.; Dawid, A. E.; Kolinski, A. Coarse-grained protein models and their applications. *Chemical Reviews* **2016**, *116*, 7898–7936.

(6) McLeish, T. Tube theory of entangled polymer dynamics. *Advances in Physics* **2002**, *51*, 1379–1527.

(7) Likhtman, A. E.; Sukumaran, S. K.; Ramirez, J. Linear viscoelasticity from molecular dynamics simulation of entangled polymers. *Macromolecules* **2007**, *40*, 6748–6757.

(8) Tassieri, M.; Evans, R.; Warren, R. L.; Bailey, N. J.; Cooper, J. M. Microrheology with optical tweezers: data analysis. *New Journal of Physics* **2012**, *14*, 115032.

(9) Mason, T.; Weitz, D. Optical measurements of frequency-dependent linear viscoelastic moduli of complex fluids. *Physical Review Letters* **1995**, *74*, 1250–1253.

(10) Mason, T. Estimating the viscoelastic moduli of complex fluids using the generalized Stokes-Einstein equation. *Rheologica acta* **2000**, *39*, 371–378.

(11) Dasgupta, B.; Tee, S.; Crocker, J.; Frisken, B.; Weitz, D. Microrheology of polyethylene oxide using diffusing wave spectroscopy and single scattering. *Physical Review E* **2002**, *65*.

(12) Evans, R. M. L.; Tassieri, M.; Auhl, D.; Waigh, T. A. Direct conversion of rheological compliance measurements into storage and loss moduli. *Physical Review E* **2009**, *80*.

(13) Evans, R. M. L. Transforming from time to frequency without artefacts. *British Society of Rheology Bulletin* **2009**, *50*, 76.

(14) Tassieri, M.; Evans, R. M. L.; Yao, A. M.; Lee, M. P.; Phillips, D. B.; Gibson, G. M.; Baule, A.; Papagiannopoulos, A.; Bowman, R. W. In *Microrheology with Optical Tweezers: Principles and Applications*; Manlio Tassieri,, Ed.; Pan Stanford, 2015.

(15) Das, A. K. Exploring the glass transition region: crowding effect, nonergodicity and thermorheological complexity. *Physical Chemistry Chemical Physics* **2015**, *17*, 16110–16124.

(16) Tassieri, M.; Laurati, M.; Curtis, D. J.; Auhl, D. W.; Coppola, S.; Scalfati, A.; Hawkins, K.; Williams, P. R.; Cooper, J. M. i-Rheo: Measuring the materials' linear viscoelastic properties "in a step"! *Journal of Rheology* **2016**, *60*, 649–660.

(17) Inoue, T.; Okamoto, H.; Osaki, K. Birefringence of amorphous polymers. 1. Dynamic measurement on polystyrene. *Macromolecules* **1991**, *24*, 5670–5675.

(18) Okamoto, H.; Inoue, T.; Osaki, K. Viscoelasticity and birefringence of polyisoprene. *Journal of Polymer Science Part B: Polymer Physics* **1995**, *33*, 417–424.

(19) Lathi, B. *Linear Systems and Signals*; Oxford Series in Electrical and Computer Engineering; Oxford University Press, USA, 2004.

(20) Ramírez, J.; Sukumaran, S. K.; Vorselaars, B.; Likhtman, A. E. Efficient on the fly calculation of time correlation functions in computer simulations. *The Journal of Chemical Physics* **2010**, *133*, 154103.

(21) Morse, D. C. Viscoelasticity of concentrated isotropic solutions of semiflexible polymers. 1. Model and stress tensor. *Macromolecules* **1998**, *31*, 7030–7043.

(22) Morse, D. C. Viscoelasticity of concentrated isotropic solutions of semiflexible polymers. 2. Linear response. *Macromolecules* **1998**, *31*, 7044–7067.

(23) Tassieri, M.; Evans, R.; Barbu-Tudoran, L.; Khaname, G. N.; Trinick, J.; Waigh, T. A. Dynamics of Semiflexible Polymer Solutions in the Highly Entangled Regime. *Physical Review Letters* **2008**, *101*, 198301.

(24) Tassieri, M. Dynamics of Semiflexible Polymer Solutions in the Tightly Entangled Concentration Regime. *Macromolecules* **2017**, *50*, 5611–5618.

(25) Reiner, M. The deborah number. *Physics today* **1964**, *17*, 62.

(26) Masubuchi, Y. Simulating the Flow of Entangled Polymers. *Annual Review of Chemical and Biomolecular Engineering* **2014**, *5*, 11–33.

(27) Masubuchi, Y. *Reference Module in Materials Science and Materials Engineering*; Elsevier, 2016; pp 1–7.

(28) Rouse, P. E. A Theory of the Linear Viscoelastic Properties of Dilute Solutions of Coiling Polymers. *The Journal of Chemical Physics* **1953**, *21*, 1272.

(29) Zimm, B. H. Dynamics of polymer molecules in dilute solution: viscoelasticity, flow birefringence and dielectric loss. *The Journal of Chemical Physics* **1956**, *24*, 269–278.

(30) Doi, M.; Edwards, S. F. *The theory of polymer dynamics*; Clarendon press: Oxford, 1986.

(31) Doi, M. Explanation for the 3.4-power law for viscosity of polymeric liquids on the basis of the tube model. *Journal of Polymer Science: Polymer Physics Edition* **1983**, *21*, 667–684.

(32) Graessley, W. W. W. *ADVANCES IN POLYMER SCIENCE*; Springer-Verlag: Berlin/Heidelberg, 1982; Vol. 47; pp 67–117.

(33) Doi, M.; Edwards, S. F. Dynamics of concentrated polymer systems. Part 1. Brownian motion in the equilibrium state. *Journal of the Chemical Society, Faraday Transactions 2* **1978**, *74*, 1789.

(34) Masubuchi, Y.; Takimoto, J.-I. I.; Koyama, K.; Ianniruberto, G.; Marrucci, G.; Greco, F. Brownian simulations of a network of reptating primitive chains. *Journal of Chemical Physics* **2001**, *115*, 4387.

(35) Uneyama, T.; Masubuchi, Y. Multi-chain slip-spring model for entangled polymer dynamics. *The Journal of Chemical Physics* **2012**, *137*, 154902.

(36) Masubuchi, Y.; Uneyama, T.; Watanabe, H.; Ianniruberto, G.; Greco, F.; Marrucci, G. Structure of entangled polymer network from primitive chain network simulations. *Journal of Chemical Physics* **2010**, *132*, 1–8.

(37) Chappa, V. C.; Morse, D. C.; Zippelius, A.; Müller, M. Translationally Invariant Slip-Spring Model for Entangled Polymer Dynamics. *Physical Review Letters* **2012**, *109*, 148302.

(38) Langeloth, M.; Masubuchi, Y.; Böhm, M. C.; Müller-plathe, F. Recovering the reptation dynamics of polymer melts in dissipative particle dynamics simulations via slip-springs. *The Journal of chemical physics* **2013**, *138*, 104907.

(39) Ramírez-Hernández, A.; Detcheverry, F. A.; Peters, B. L.; Chappa, V. C.; Schweizer, K. S.; Müller, M.; de Pablo, J. J. Dynamical Simulations of Coarse Grain Polymeric Systems: Rouse and Entangled Dynamics. *Macromolecules* **2013**, *46*, 6287–6299.

(40) Masubuchi, Y.; Langeloth, M.; Böhm, M. C.; Inoue, T.; Müller-Plathe, F. A Multichain Slip-Spring Dissipative Particle Dynamics Simulation Method for Entangled Polymer Solutions. *Macromolecules* **2016**, *49*, 9186–9191.

(41) Schwarzl, F. Numerical calculation of storage and loss modulus from stress relaxation data for linear viscoelastic materials. *Rheologica Acta* **1971**, *10*, 165–173.

(42) Matsumiya, Y.; Kumazawa, K.; Nagao, M.; Urakawa, O.; Watanabe, H. Dielectric Relaxation of Monodisperse Linear Polyisoprene: Contribution of Constraint Release. *Macromolecules* **2013**, *46*, 6067–6080.

(43) Masubuchi, Y.; Amamoto, Y.; Pandey, A.; Liu, C.-Y. Primitive chain network simulations of probe rheology. *Soft Matter* **2017**, *13*, 6585–6593.

(44) Kremer, K.; Grest, G. S. Dynamics of entangled linear polymer melts: A molecular-dynamics simulation. *The Journal of Chemical Physics* **1990**, *92*, 5057–5086.

(45) Auhl, R.; Everaers, R.; Grest, G. S.; Kremer, K.; Plimpton, S. J. Equilibration of long chain polymer melts in computer simulations. *The Journal of chemical physics* **2003**, *119*, 12718–12728.

(46) Sukumaran, S. K.; Likhtman, A. E. Modeling entangled dynamics: comparison between stochastic single-chain and multichain models. *Macromolecules* **2009**, *42*, 4300–4309.

(47) Wang, Z.; Likhtman, A. E.; Larson, R. G. Segmental Dynamics in Entangled Linear Polymer Melts. *Macromolecules* **2012**, *45*, 3557–3570.

(48) van der Ploeg, P.; Berendsen, H. J. C. Molecular dynamics simulation of a bilayer membrane. *The Journal of Chemical Physics* **1982**, *76*, 3271–3276.

(49) Toxvaerd, S. Equation of state of alkanes II. *The Journal of Chemical Physics* **1997**, *107*, 5197–5204.

(50) Martin, M. G.; Siepmann, J. I. Transferable potentials for phase equilibria. 1. United-atom description of n-alkanes. *The Journal of Physical Chemistry B* **1998**, *102*, 2569–2577.

(51) Karayiannis, N. C.; Mavrantzas, V. G.; Theodorou, D. N. A Novel Monte Carlo Scheme for the Rapid Equilibration of Atomistic Model Polymer Systems of Precisely Defined Molecular Architecture. *Physical Review Letters* **2002**, *88*.

(52) Karayiannis, N. C.; Giannousaki, A. E.; Mavrantzas, V. G.; Theodorou, D. N. Atomistic Monte Carlo simulation of strictly monodisperse long polyethylene melts through a generalized chain bridging algorithm. *The Journal of Chemical Physics* **2002**, *117*, 5465–5479.

(53) Nosé, S. A molecular dynamics method for simulations in the canonical ensemble. *Molecular Physics* **1984**, *52*, 255–268.

(54) Hoover, W. G. Canonical dynamics: Equilibrium phase-space distributions. *Physical Review A* **1985**, *31*, 1695–1697.

(55) Tuckerman, M.; Berne, B. J.; Martyna, G. J. Reversible multiple time scale molecular dynamics. *The Journal of Chemical Physics* **1992**, *97*, 1990–2001.

(56) Plimpton, S. Fast Parallel Algorithms for Short-Range Molecular Dynamics. *Journal of Computational Physics* **1995**, *117*, 1–19.

(57) Karayiannis, N. C.; Mavrantzas, V. G. Hierarchical modeling of the dynamics of polymers with a nonlinear molecular architecture: Calculation of branch point friction and chain reptation time of H-shaped polyethylene melts from long molecular dynamics simulations. *Macromolecules* **2005**, *38*, 8583–8596.

(58) Likhtman, A.; McLeish, T. Quantitative theory for linear dynamics of linear entangled polymers. *Macromolecules* **2002**, *35*, 6332–6343.

(59) Fetters, L. J.; Lohse, D. J.; Richter, D.; Witten, T. A.; Zirkel, A. Connection between Polymer Molecular Weight, Density, Chain Dimensions, and Melt Viscoelastic Properties. *Macromolecules* **1994**, *27*, 4639–4647.

# Graphical TOC Entry